

Supporting Information

Self-assembled hybrid organic-MoS₃-nanoparticle catalyst for light energy conversion

EXPERIMENTAL SECTION

Chemicals. Sodium molybdate dihydrate (Na₂MoO₄) was obtained from Merck with an analytical grade of 99.5%. Thioacetamide was purchased from Riedel AG Haen AG with an analytical grade of 98%. Poly(styrene sulfonate) sodium salt (PSS) with an average molar weight of 450,000 and a polydispersity index *PDI* < 1.2 was supplied from PSS Polymer Standards Service and Poly(diallyldimethylammonium chloride) (PDADMAC) solution as 20 wt.% in water with an average molar weight of $M_w = 200,000$ to 350,000 was supplied from Sigma-Aldrich. Methyl red was purified by recrystallization to yield a dye content of $\approx 100\%$. To prepare samples and stock solutions, deionized water was used, which was filtered through two hydrophilic PTFE filters of a pore size of 0.2 μm . The pH was adjusted with a 1 mol L⁻¹ hydrochloric acid from AVS Titrimorm (VWR Chemicals).

Preparation of Polymer-MoS₃-Aggregates. Stock solutions of the polymers and Na₂MoO₄ were prepared by dissolving an appropriate amount of substance in neutral deionized filtered water to yield an exact concentration. For the samples, an appropriate amount of polymer was added to water at pH 3, then Na₂MoO₄ stock solution was added while stirring. The thioacetamide stock solution was freshly prepared by dissolving thioacetamide in equal part of water and 1 N hydrochloric acid, and then added to the polymer-MoO₄²⁻ solution while stirring. After 30 min stirring, the samples were ultrasonicated at 60° C until the samples turned from colorless to blue (isopolymolbdates) to brown color. The samples were stirred for 15 h at room temperature. The reference system with MoS₃ only was prepared equally with replacing the amount of polymer stock solution with water. Previous computer studies using Monte Carlo showed that amorphous MoS₃ yields the structure Mo^{IV}S₂⁻ S²⁻. In MoS₃, sulfur is present in two states so that the molybdenum in Na₂MoO₄ is reduced in MoS₃.^[47]

For catalysis, the samples were dissolved to obtain a MoS₃ concentration of $c(\text{MoS}_3) = 1.9 \cdot 10^{-4}$ mol L⁻¹ and the excess of in situ generate H₂S of thioacetamide were removed with air. As hole scavenger freshly prepared thioacetamide solution was added to achieve a concentration of $c(\text{thioacetamide}) = 8.3 \cdot 10^{-3}$ mol L⁻¹. Then dye stock solution was added, which was prepared by dissolving an appropriate amount of methyl red in deionized water. The irradiation was performed with a 300 W halogen lamp from esylux with a visible spectrum similar to daylight and the time measure starts when adding methyl red to the sample.

Light Scattering. Light scattering experiments were performed on an ALV CGS 3 goniometer with ALV 5000 correlator (ALV Langen, Germany) equipped with a HeNe laser with a wavelength of $\lambda = 632.8$ nm and 20 mW output power. For dynamic light scattering an angular range of $30^\circ \leq \vartheta \leq 150^\circ$ is measured in 10° steps. The electric field autocorrelation $g^1(q, \tau)$ was calculated from the resulting intensity autocorrelation function $g^2(q, \tau)$ by the Siegert relation. After that, $g^1(q, \tau)$ was analyzed by inverse LaPlace transformation using the program CONTIN by S. Provencher⁶² to yield the distribution of relaxation times $A(\tau)$. Based on this, the apparent diffusion coefficients D_{app} could be calculated for each particle species separately. The diffusion coefficient D was obtained by plotting D_{app} against q^2

and subsequent extrapolation to zero. This diffusion coefficient was then converted into the hydrodynamic radius R_H via the Stokes-Einstein relationship. In static light scattering, the average sample, solvent (water) and standard (toluene) scattering intensity were recorded in dependence on the scattering angle.

UV/Vis Spectroscopy. UV/Vis spectra were recorded with a UV/Vis spectrometer UV 1800 from SHIMADZU. The slit width was 1 nm and quartz cuvettes from Hellma/Müllheim with 10 cm path length were used to investigate samples in a spectral range reached of $200 \text{ nm} \leq \lambda \leq 1000 \text{ nm}$.

Atomic Force Microscopy (AFM). AFM samples were prepared by drop casting the samples on freshly cleaved mica and blow-dried after 10 min incubation. AFM images were recorded in air with an AFM from NanoSurf (Boston, USA) in non-contact mode and 512 measuring points per line. The time/line result was adjusted to 0.5 s with a loop-gain of 11. The images were analysed with the software WSxM 4.0 Beta 7.0.^[48] Due the small height of the polymer-MoS₃ aggregates in comparison to the lateral diameter the volumes of the AFM structures were calculated. A spherical cap was assumed as model for the AFM structures, while for volume calculation in solution a sphere with $r = R_H$ was used for calculation.

Scanning Electron Microscopy (SEM). SEM micrographs were obtained on a Jeol JSM 6400 PC equipped with a LaB₆ cathode at acceleration voltages 10 kV. For the SEM polymer-MoS₃ samples with $c(\text{MoS}_3) = 2.0 \cdot 10^{-5} \text{ mol L}^{-1}$ were drop-casted on an electrochemically polished copper platelet and dried at 50°C. Due the poor electrical conductivity of the polymer a $5 \text{ nm} \pm 1 \text{ nm}$ gold layer was deposited with DC/HF sputter coater from Torr.

Transmission Electron Microscopy (TEM). The TEM images were acquired with a Zeiss EM 900 microscope, operated at 80 kV at magnifications ranging from 20 000 to 250 000. The specimens were prepared by depositing 5mL of the diluted sample solution onto carbon-coated copper grids, 300 mesh, and air-dry the grids.

RAMAN spectroscopy. Experiments were carried out with an amplified Ti:Sapphire CPA-2110 fs laser system (Clark MXR: output 775 nm, 1 kHz, 150 fs pulse width) using transient absorption pump/probe detection systems (Helios and Eos, Ultrafast Systems) with nitrogen purged solutions. The excitation wavelength was generated with a noncolinear optical parametric amplifier (NOPA, Clark MXR).

Light microscopy. The light microscopy images were obtained with a Leica DM 4000 M microscope operated with transmitted light at magnifications of 20 x and a Leica DFC 320 digital camera.

ADDITIONAL RESULTS

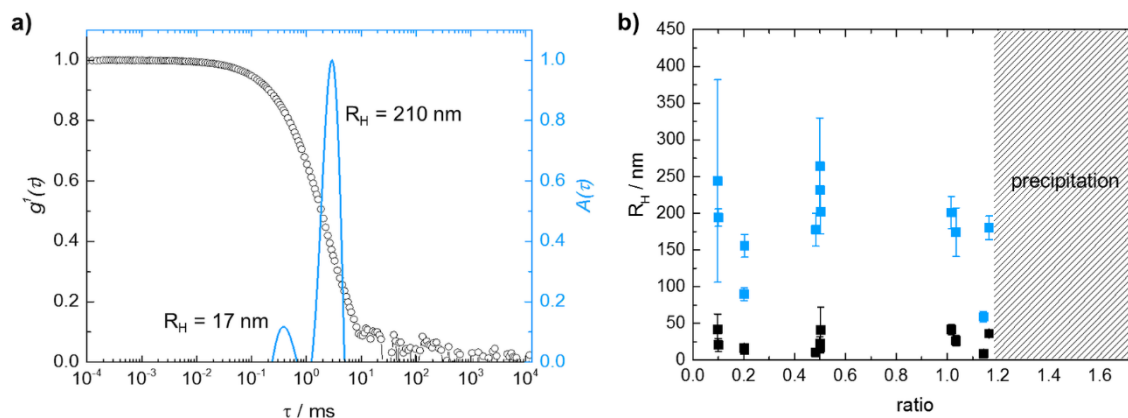


Figure S1: Dynamic light scattering results of PDADMAC-MoS₃ assemblies at pH 2.5 depending on the ratio r , a) electric field autocorrelation function $g^1(\tau)$ (black) and distribution of relaxation times $A(\tau)$ (blue) at a scattering angle $\vartheta = 90^\circ$; b) larger and smaller R_H of PDAMAC-MoS₃ assemblies depending on the ratio r ; $c(\text{MoS}_3) = 5.0 \cdot 10^{-3} \text{ mol L}^{-1}$.

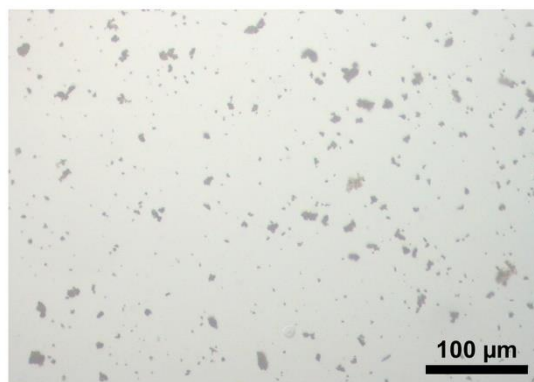


Figure S2: a) Light microscope image of MoS₃ particles synthesized without polymer used as reference for the determination of the catalytic activity: polydisperse particle with a diameter $d < 30 \mu\text{m}$.

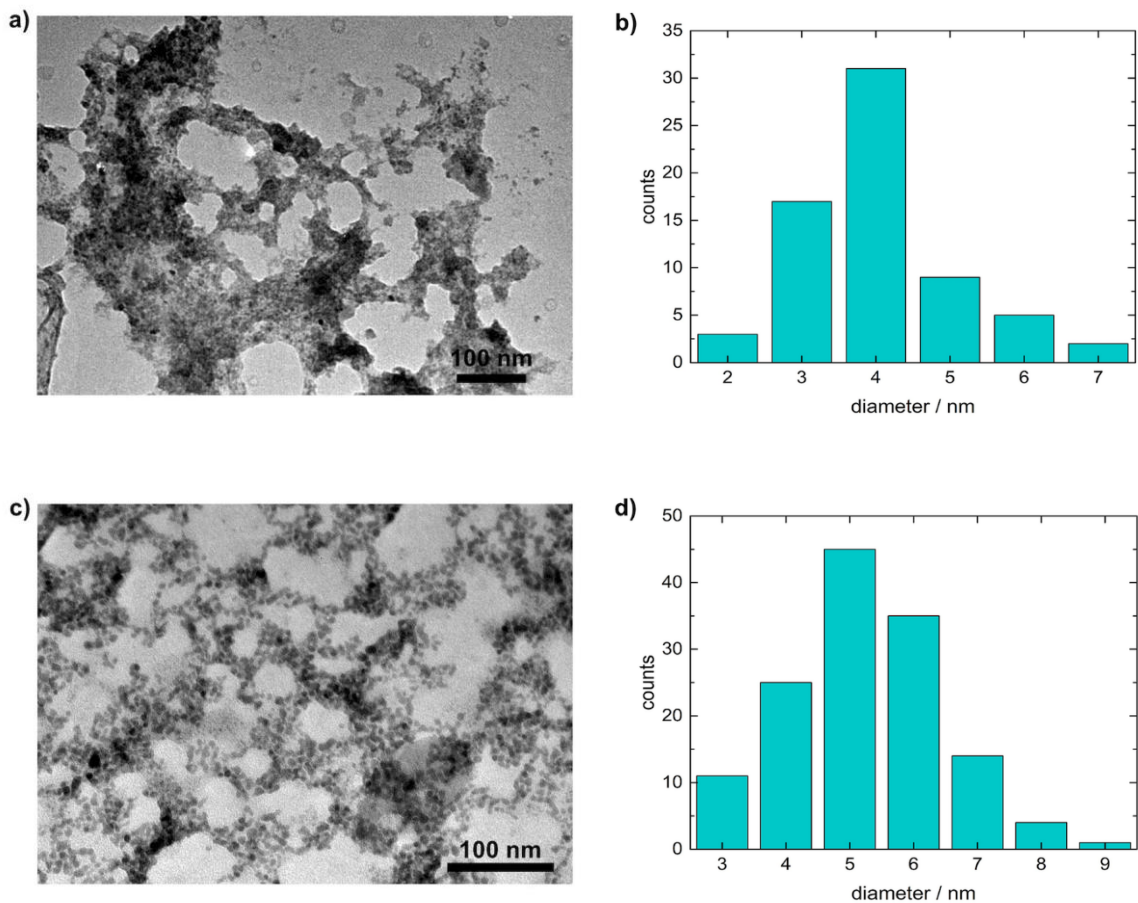


Figure S3: a) TEM image of PDADMAC-MoS₃ assemblies with $r = 0.1$ with b) corresponding statistics for the MoS₃ nanoparticles; c) TEM image of network-like PDADMAC-MoS₃ assemblies with $r = 0.5$ with d) corresponding statistics for the MoS₃ nanoparticles.

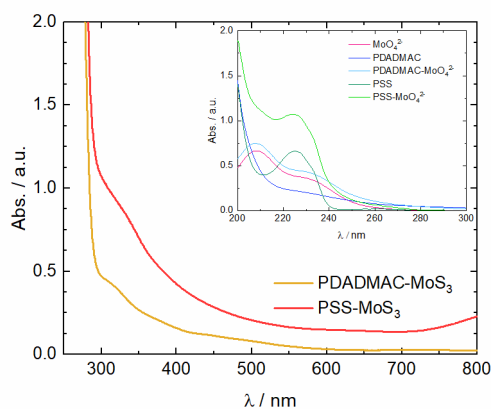


Figure S4: UV-vis spectra of PDADMAC-MoS₃ and PSS-MoS₃: both samples show absorption over the wavelength range; inset: UV-spectra of the educts.

Due to the absorption of the polymers and the variation of the MoS₃ structural configurations the band gap determination is not possible.

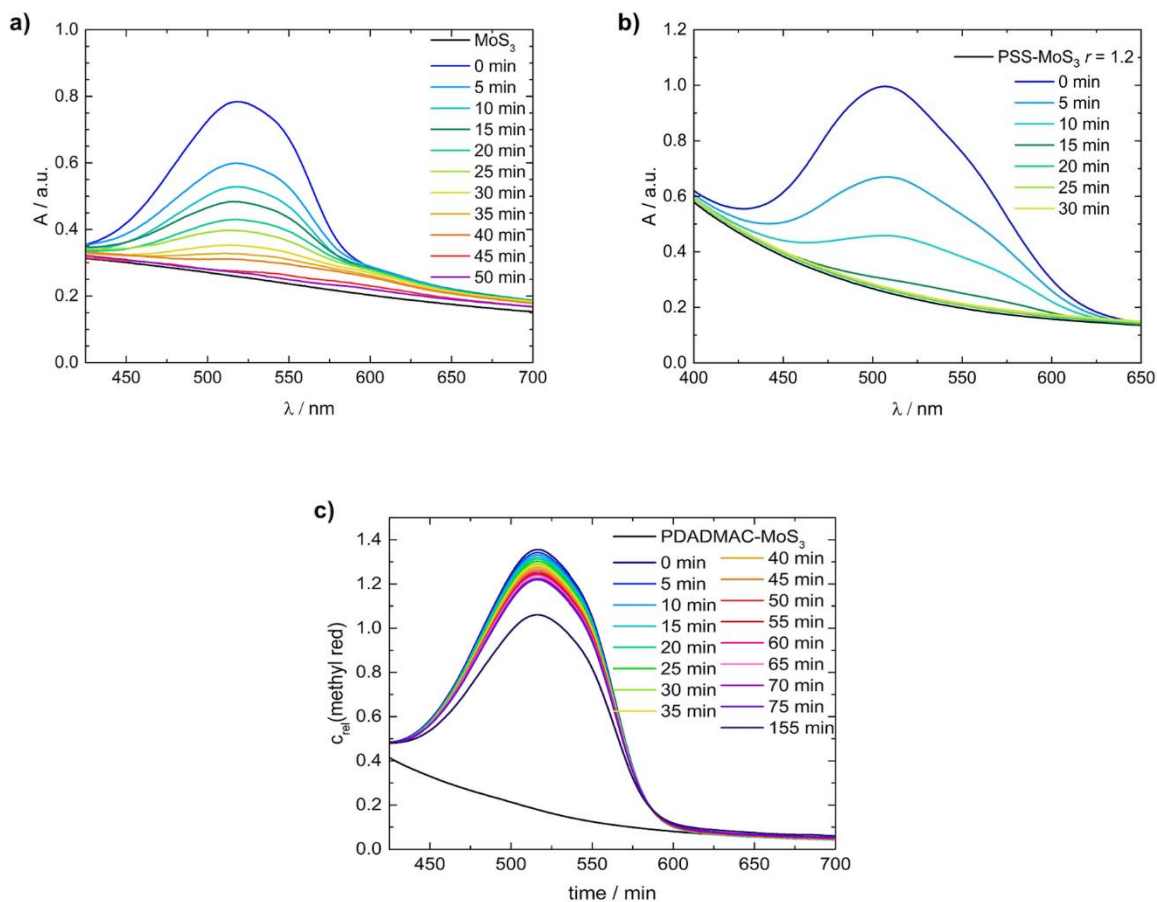


Figure S5: UV/Vis spectra of the methyl red degradation upon irradiation with visible light measured at $\lambda = 508$ nm with thioacetamide ($c(\text{thioacetamide}) = 8.3 \cdot 10^{-3} \text{ mol L}^{-1}$) as hole scavenger; a) MoS₃, b) PDADMAC-MoS₃ assemblies with $r = 1.2$ and c) PSS-MoS₃ assemblies as photocatalyst; each sample contains a MoS₃ concentration of $c(\text{MoS}_3) = 2.0 \cdot 10^{-4} \text{ mol L}^{-1}$.

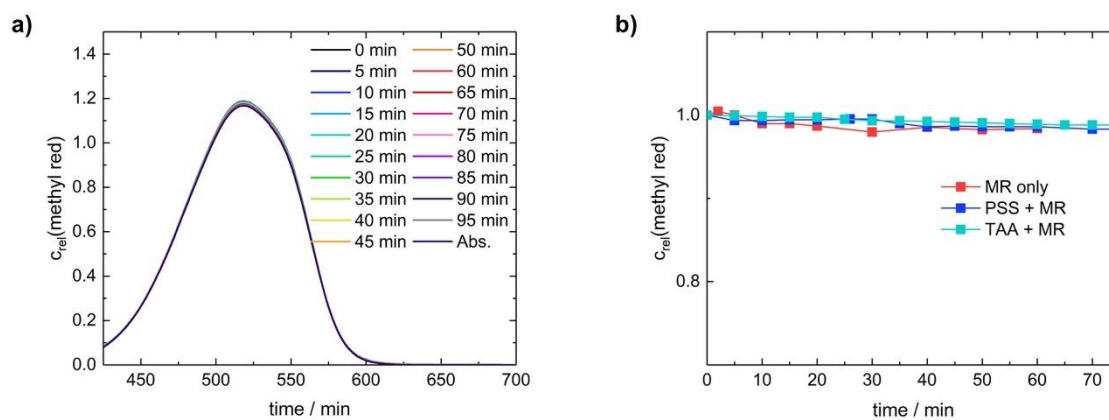


Figure S6: Photocatalytic activity: a) UV/Vis spectra of the methyl red degradation upon irradiation with visible light measured at $\lambda = 508$ nm in the presence of thioacetamide ($c(\text{thioacetamide}) = 8.3 \cdot 10^{-3} \text{ mol L}^{-1}$); b)

Behaviour of the methyl red photodegradation upon irradiation with visible light measured at $\lambda = 508$ nm without MoS₃.

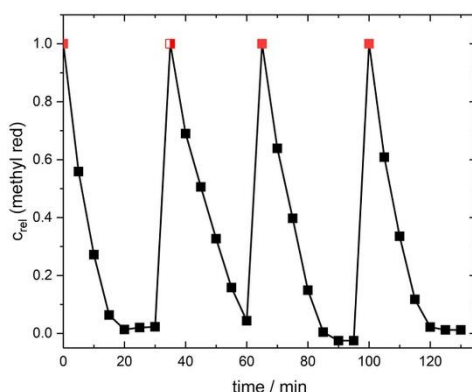


Figure S7: Photocatalytic activity of PSS-MoS₃ with $r = 1.2$ during four reaction cycles measured at $\lambda = 508$ nm: the red square marks the beginning of a reaction cycle; each cycle 100 μ l thioacetamide ($c(\text{thioacetamide}) = 8.3 \cdot 10^{-3} \text{ mol L}^{-1}$) and 45 μ l of methyl red ($c(\text{methyl red}) = 1.5 \cdot 10^{-3} \text{ mol L}^{-1}$) were added to the sample; for the second reaction cycle no thioacetamide was added (red half square).

Table S1: Summary and comparison of the photocatalytic activity: degradation of azo-dyes by MoS_x.

sample	r	$c(\text{thioacetamide})$ [mol L ⁻¹]	$c(\text{MoS}_3)$ [mol L ⁻¹]	degradation of methyl red after 15 min	complete degradation	dye
MoS ₃	-	$8.3 \cdot 10^{-3}$	$1.9 \cdot 10^{-4}$	57.3 %	45 min	methyl red
PDADMAC-MoS ₃	1.2	$8.3 \cdot 10^{-3}$	$1.9 \cdot 10^{-4}$	2.9 %	> 10 h	methyl red
PSS-MoS ₃	3	$8.3 \cdot 10^{-3}$	$1.9 \cdot 10^{-4}$	100 %	15 min	methyl red
PSS-MoS ₃	1.2	$8.3 \cdot 10^{-3}$	$1.9 \cdot 10^{-4}$	93.7 %	20 min	methyl red
PSS-MoS ₃	0.7 5	$8.3 \cdot 10^{-3}$	$1.9 \cdot 10^{-4}$	31.9 %	55 min	methyl red
PSS-MoS ₃	0.5	$8.3 \cdot 10^{-3}$	$1.9 \cdot 10^{-4}$	33.3 %	50 min	methyl red
MoS ₂ /C ₃ N ₄ ^[45]	Heterogeny catalyst, 0.05 wt % MoS ₂		-	2 % - 15 %	> 3.5 h - 10 h	methyl orange
CoFe ₂ O ₄ /MoS ₂ ^[46]	Heterogeny catalyst, Co/Mo = 0.5,		$2.0 \cdot 10^{-3}$	34 %	> 2h	Congo red
CoFe ₂ O ₄ /MoS ₂ ^[46]	Heterogeny catalyst, Co/Mo = 1.0		$2.0 \cdot 10^{-3}$	45 %	> 60 min	Congo red
CoFe ₂ O ₄ /MoS ₂ ^[46]	Heterogeny catalyst, Co/Mo = 2.0		$2.0 \cdot 10^{-3}$	41 %	> 2h	Congo red
CoFe ₂ O ₄ /MoS ₂ ^[46]	Heterogeny catalyst, Co/Mo = 1.0		$2.0 \cdot 10^{-3}$	43 %	> 60 min	methyl orange

[45] Q. Li, N. Zhang, Y. Yang, G. Wang and Ng, Dickon H L, *Langmuir* 2014, **30**, 8965–8972.

[46] B. Ren, W. Shen, L. Li, S. Wu and W. Wang, *Appl. Surf. Sci.* 2018, **447**, 711-723.

[47] S. J. Hibble and G. B. Wood, *J. Am. Chem. Soc.* 2004, **126**, 959.

[48] I. Horcas, R. Fernández, J. M. Gómez-Rodríguez, J. Colchero, J. Gómez-Herrero and A. M. Baro, *Rev. Sci. Instrum.* 2007, **78**, 13705.